Identification of a signaling cascade that maintains constitutive δ-opioid receptor incompetence in peripheral sensory neurons

Allison Doyle Brackley[‡]**, Shayda Sarrami**[§]**, Ruben Gomez**[§]**, Kristi A. Guerrero**[§]**, and Nathaniel A. Jeske**[‡§¶1]

From the Departments of [‡]*Pharmacology,* [§]*Oral and Maxillofacial Surgery, and* [¶]*Physiology, University of Texas Health Science Center, San Antonio, Texas 78229*

Edited by Henrik G. Dohlman

μ-Opioid receptor (MOR) agonists are often used to treat severe pain but can result in adverse side effects. To circumvent systemic side effects, targeting peripheral opioid receptors is an attractive alternative treatment for severe pain. Activation of the δ-opioid receptor (DOR) produces similar analgesia with reduced side effects. However, until primed by inflammation, peripheral DOR is analgesically incompetent, raising interest in the mechanism. We recently identified a novel role for G-protein-coupled receptor kinase 2 (GRK2) that renders DOR analgesically incompetent at the plasma membrane. However, the mechanism that maintains constitutive GRK2 association with DOR is unknown. Protein kinase A (PKA) phosphorylation of GRK2 at Ser-685 targets it to the plasma membrane. Protein kinase A-anchoring protein 79/150 (AKAP), residing at the plasma membrane in neurons, scaffolds PKA to target proteins to mediate downstream signal. Therefore, we sought to determine whether GRK2-mediated DOR desensitization is directed by PKA via AKAP scaffolding. Membrane fractions from cultured rat sensory neurons following AKAP siRNA transfection and from AKAP-knock-out mice had less PKA activity, GRK2 Ser-685 phosphorylation, and GRK2 plasma membrane targeting than controls. Site-directed mutagenesis revealed that GRK2 Ser-685 phosphorylation drives the association of GRK2 with plasma membrane-associated DOR. Moreover, overexpression studies with AKAP mutants indicated that impaired AKAP-mediated PKA scaffolding significantly reduces DOR-GRK2 association at the plasma membrane and consequently increases DOR activity in sensory neurons without a priming event. These findings suggest that AKAP scaffolds PKA to increase plasma membrane targeting and phosphorylation of GRK2 to maintain DOR analgesic incompetence in peripheral sensory neurons.

Systemic opioid therapies that target the μ-opioid receptor (MOR)[2] remain the gold standard for the treatment of acute severe pain. Although highly efficacious as an analgesic strategy, debilitating systemic side effects contraindicate long-term use, including respiratory depression, dependence, and addiction (1). Targeting the δ-opioid receptor (DOR), on the other hand, produces comparable analgesia with reduced side-effect profiles in rodents and non-human primates (2). Recent studies have also demonstrated that activation of competent opioid receptors in the periphery adequately relieve pain to the same extent as central administration (3). However, agonist activation of peripheral opioid receptors, including DOR, requires an inflammatory prestimulus or "priming" event (4–11). Peripheral DOR incompetence is maintained by a constitutive interaction between the receptor and G-protein-coupled receptor kinase 2 (GRK2) (11). Exposure to inflammatory mediator bradykinin induces a "priming" cascade that involves protein kinase C (PKC)-induced phosphorylation of Raf-kinase-inhibitory protein (RKIP), followed by RKIP self-dimerization and GRK2 sequestration to the cytosol. The mechanism for opioid analgesic incompetence is not well understood and could provide important insight into the role of inflammatory mediators in peripheral opioid receptor regulation.

Protein kinase A (PKA), the primary kinase target for cAMP, is an enzyme consisting of two catalytic (C) subunits rendered inactive by dimerized regulatory (R) subunits (12–14). PKA isoforms differ in their R subunits, RI and RII (15–17). High-affinity interactions between intracellular targeting domains in protein kinase A-anchoring protein 79/150 (AKAP) and PKA RII anchor PKA to the plasma membrane, allowing for spatial and temporal regulation of target proteins (18, 19). Interestingly, genetic ablation of AKAP or disruption of PKA scaffolding by AKAP in mice reduces postsynaptic PKA localization in brain lysates (20–22). In the periphery, immunohistochemical analysis of intact and cultured rat trigeminal ganglia (TG) reveal neuronal coexpression of AKAP and PKA RII (23). Comple-

[1] To whom correspondence should be addressed: Dept. of Oral and Maxillofacial Surgery, University of Texas Health Science Center at San Antonio School of Dentistry, 7703 Floyd Curl Dr., San Antonio, TX 78229. Tel.: 210-567-3466; Fax: 210-567-2995; E-mail: Jeske@uthscsa.edu.

[2] The abbreviations used are: MOR, μ-opioid receptor; DOR, δ-opioid receptor; GRK2, G-protein-coupled receptor kinase 2; RKIP, Raf-kinase-inhibitory protein; AKAP, protein kinase A-anchoring protein 79/150; TG, trigeminal ganglia; DRG, dorsal root ganglia; ANOVA, analysis of variance; 8-Br-cAMP, 8-bromo-cyclic AMP; VGCG, voltage-gated Ca^{2+} channels; CAP, capsaicin; DPDPE, [D-Pen^{2,5}]enkephalin; IP, immunoprecipitation; PM, plasma membrane; EV, empty vector; SES, standard extracellular solution; WB, Western blotting.

ASBMB

mentary biochemical analysis in cultured TG lysates reveals that AKAP co-immunoprecipitates with PKA RII. In immortalized cells, AKAP scaffolding of PKA drives GRK2 to the plasma membrane, where it modulates G-protein-coupled receptors (GPCRs) (24).

In the present study, we investigate the potential role of AKAP scaffolding of PKA in constitutive GRK2 maintenance of DOR incompetence in peripheral sensory neurons. Using imaging, biochemical, molecular, and functional techniques, we sought to determine whether AKAP scaffolding of PKA sustains GKR2-DOR association and functional receptor incompetence in the periphery. Such a mechanism could be used to identify novel drugs that disrupt these protein-protein interactions for use in combination therapy with peripherally restricted DOR agonists. This approach would be expected to enhance DOR-mediated analgesia in non-inflammatory pain patients with a reduced likelihood of systemic side effects.

Results

AKAP enhances PKA activity at the plasma membrane

Previous studies have demonstrated that AKAP serves to anchor PKA RII to the plasma membrane (19, 25). In central tissues, genetic ablation of AKAP or disruption to AKAP scaffolding of PKA reduces postsynaptic PKA RII localization (20–22). In the periphery, immunohistochemical analysis of intact and cultured rat TG revealed neuronal co-expression of AKAP and PKA RII (23). To determine whether AKAP plays a role in membrane localization of PKA RII in the periphery, qualitative confocal microscopy was utilized to examine PKA RII distribution across cultured TG and dorsal root ganglia (DRG) from AKAP wild-type (WT) and knock-out (KO) mice (Fig. 1A). PKA RII is well-distributed throughout the TG and DRG of WT mice and, to a lesser extent, KO mice. Although whole-cell PKA RII densitometry across groups does not significantly differ, PKA RII is significantly increased at the plasma membrane of WT TG and DRG compared with KO neurons (Fig. 1B, (whole-cell) interaction, $p = 0.8599$; (whole-cell) WT *versus* KO, $p = 0.6133$; (whole-cell) TG *versus* DRG, $p = 0.0501$; ((plasma membrane; PM) interaction, $p = 0.1769$; (PM) WT *versus* KO, $p = 0.0527$; (PM) TG *versus* DRG, $p = 0.1000$; $n = 41–77$; two-way ANOVA with Bonferroni post hoc test). This interaction was confirmed when plasma membrane PKA RII was compared with total PKA RII for each group (Fig. 1C, interaction, $p = 0.0271$; TG *versus* DRG, $p = 0.0063$; WT *versus* KO, $p < 0.0001$; $n = 41–77$; two-way ANOVA with Bonferroni post hoc test). Compared with WT, the percentage of PKA RII at the plasma membrane in KO neurons is reduced by $58.27 \pm 9.34\%$ in TG and $42.36 \pm 14.95\%$ in DRG. These data identify that AKAP supports PKA localization at the plasma membrane in peripheral sensory neurons.

We next employed an *in vitro* assay to assess kinase activity in membrane fractions of intact or cultured TG to determine the role of AKAP in local PKA activity at the plasma membrane in mice and rats. Compared with WT mice, PKA activity in membrane lysates of AKAP KO mice is reduced by $50.24 \pm 12.31\%$ (Fig. 1D, $p = 0.0009$, $n = 3$ independent trials in triplicate,

unpaired Student's t test). As previously reported, AKAP siRNA treatment to cultured rat TG does not change PKA activity of whole-cell lysates as measured by Western blotting (WB) (23). However, transfection of rat TG cultures with AKAP siRNA significantly reduces PKA activity at the plasma membrane by $33.73 \pm 9.79\%$ compared with mock treatment (Fig. 1E, $p = 0.0033$, $n = 3$ independent trials in triplicate, unpaired Student's t test). Collectively, these data suggest that AKAP serves to anchor active PKA to the plasma membrane in peripheral sensory neurons of both mice and rats.

AKAP facilitates PKA-dependent GRK2 phosphorylation

In immortalized cells, PKA activation stimulates phosphorylation of numerous proteins, including the direct phosphorylation GRK2 at Ser-685 (24). Although PKA phosphorylation of GRK2 does not enhance GRK2 catalytic activity, it facilitates GRK2 modulation of GPCRs by targeting GRK2 to the plasma membrane.

We sought to determine whether this mechanism occurs in peripheral sensory neurons. To determine whether PKA activation leads to direct PKA phosphorylation of GRK2, we utilized a phosphorylation site-specific antibody for GRK2 at Ser-685 (Fig. 2, A and B). Serum-starved rat TG cultures were stimulated with 8-Br-cAMP (10 μM; 5 min), followed by homogenization and crude fractionation. Next, GRK2 was isolated from cytosol and membrane lysates by immunoprecipitation. Stimulation by 8-Br-cAMP significantly increases PKA-dependent GRK2 phosphorylation by $278.00 \pm 80.42\%$ in the cytosol, whereas PKA stimulation resulted in a trend toward increased PKA-dependent phosphorylation by $147.80 \pm 58.43\%$ at the plasma membrane (Fig. 2, A and B; $p = 0.0259$ (A) and $p = 0.0647$ (B), $n = 3$ independent trials, unpaired student's t test). Compared with vehicle-treated cells, 8-Br-cAMP treatment also resulted in a trend toward increased GRK2 translocation to the plasma membrane by $61.60 \pm 22.35\%$ (Fig. 2C, $p = 0.0511$, $n = 3$ independent trials, unpaired Student's t test). This experiment recapitulates what was found in immortalized cells and reveals that stimulation of PKA enhances PKA-dependent phosphorylation in the cytosol and, albeit just beyond significance, may have similar effects at the plasma membrane as a result of translocation of GRK2 in rat primary sensory neurons.

AKAP scaffolding of PKA indirectly regulates GRK2 membrane translocation in immortalized cells, which requires PKA to be tethered to the plasma membrane (24). In cultured rat TG lysates, that AKAP co-immunoprecipitates with PKA RII (23). However, it has yet to be determined whether AKAP can indirectly regulate PKA-dependent phosphorylation and translocation of GRK2 in primary sensory neurons. For this experiment, we harvested and fractionated serum-starved rat TG cultures that had been transfected either in mock fashion or with AKAP siRNA. Knockdown of AKAP did not reduce PKA-dependent GRK2 phosphorylation in the cytosol (Fig. 2D, $p = 0.3292$, $n = 3$ independent trials, unpaired Student's t test). However, AKAP knockdown significantly reduces membrane GRK2 phosphorylation at Ser-685 by $39.32 \pm 15.48\%$ and is accompanied by a reduction in GRK2 membrane targeting by $44.22 \pm 18.71\%$ (Fig. 2, E and F; $p = 0.0441$ (E) and $p = 0.0560$ (F), $n = 3$
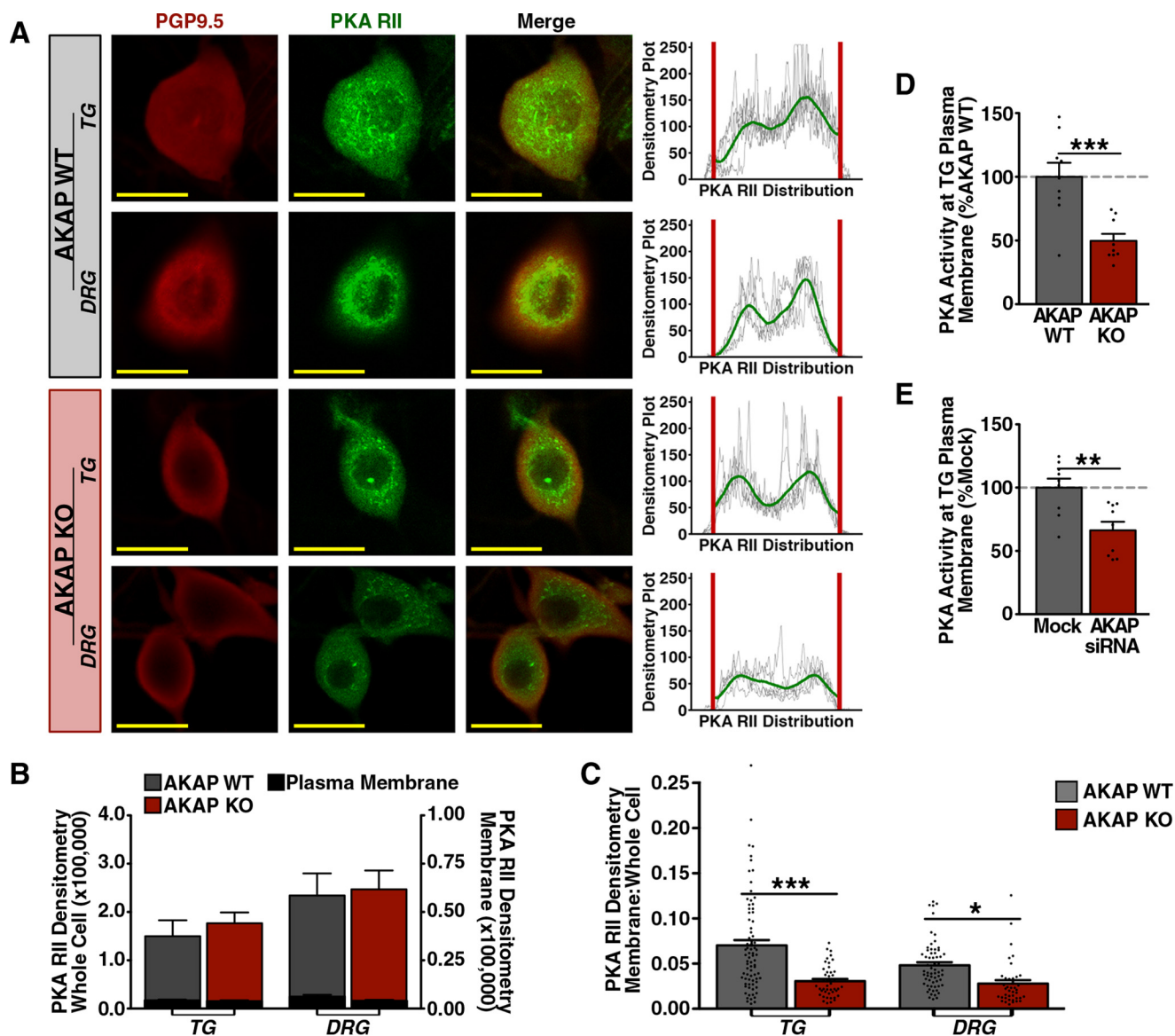
Figure 1. AKAP effect on PKA cellular distribution and PKA activity at the plasma membrane in sensory neurons. *A,* immunohistochemical co-expression of PGP9.5 (*red*) and PKA RII (*green*) in TG and DRG cultured from naive AKAP WT and AKAP KO littermates. *Yellow scale bar,* 25 μM. PKA RII distribution of representative cells is shown in the *right column*: second order smoothing polynomial (*green*) of six individual plot profiles measured with 60° separations (*gray*) near the cell membrane (*red*). Confocal images are representative of three independent trials. *B,* PKA RII densitometry measurements taken from whole cell (*left y axis*) and plasma membrane (*right y axis*, *black bars*) of TG and DRG from AKAP WT (*dark gray*) and AKAP KO (*red*). $n = 41$–77 neurons/group. *C,* PKA RII plasma membrane/whole cell densitometry ratios from AKAP WT (*gray*) and AKAP KO (*red*) TG and DRG (from *B*). $n = 41$–77 neurons/group; *, $p < 0.05$; ***, $p < 0.005$; two-way ANOVA with Bonferroni post-hoc test. *D,* PKA activity at the plasma membrane in homogenized TG from AKAP WT (*gray*) and AKAP KO (*red*) mice. $n = 3$ independent trials performed in triplicate. ***, $p < 0.005$; unpaired Student's *t* test. *E,* PKA activity at plasma membrane in rat TG cultures treated in mock fashion (*gray*) or with AKAP siRNA (*red*). $n = 3$ independent trials performed in triplicate; **, $p < 0.01$; unpaired Student's *t* test. *Error bars,* S.E.

independent trials, unpaired Student's *t* test). Similarly, crude membrane TG lysates from AKAP KO mice have $31.10 \pm 9.47\%$ less PKA-dependent GRK2 phosphorylation than WT littermates (Fig. 2*G*, $p = 0.0304$, $n = 3$ independent trials, unpaired Student's *t* test). Importantly, GRK2 targeting to the plasma membrane in AKAP KO TG is significantly reduced by $26.75 \pm 9.54\%$ compared with WT littermates (Fig. 2*H*, $p = 0.0485$, $n = 3$ independent trials, unpaired Student's *t* test). These experiments agree with the aforementioned study in immortalized cells and demonstrate that AKAP expression is crucial to constitutive PKA-dependent phosphorylation of GRK2 targeted to the membrane in rat peripheral sensory neurons.

PKA phosphorylation of GRK2 drives association with DOR

Under non-inflammatory conditions, DOR is chronically bound to GRK2, which renders the receptor dormant or unresponsive to agonist stimulation in peripheral sensory neurons (11). In immortalized cells, phosphorylation by PKA facilitates GRK2 translocation to the plasma membrane to negatively modulate GPCR signaling (24). Given that PKA-dependent phosphorylation dictates plasma membrane translocation of GRK2 (Fig. 2), we hypothesized that PKA-dependent phosphorylation of GRK2 may underlie the constitutive association between DOR and GRK2 at the plasma membrane in primary sensory neurons. To test this, we utilized site-directed mutagenesis.
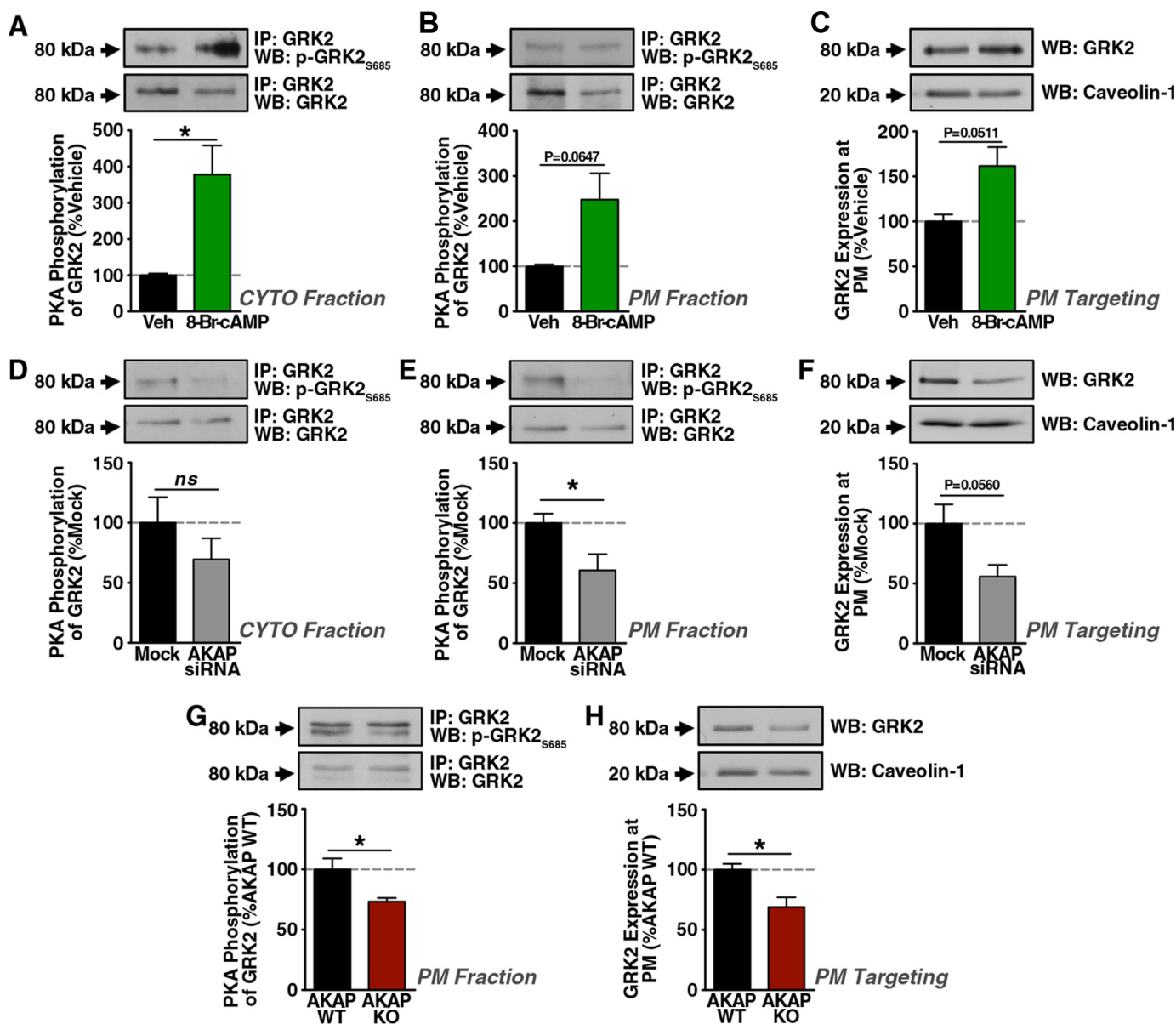
Figure 2. AKAP facilitates PKA-dependent GRK2 phosphorylation and targets GRK2 to PM. *A* and *B*, crude cytosolic (*CYTO*) and PM fraction immunoprecipitations from TG cultures serum-starved for 18 h and treated with vehicle (*black*) and 8-Br-cAMP (*green*; 10 μM, 5 min). *C*, additional crude membrane samples were collected to examine GRK2 expression at the PM. *D* and *E*, crude cytosolic and PM fraction immunoprecipitations from TG cultures treated in mock fashion (*black*) or with AKAP siRNA (*gray*) and serum-starved for 4 h. *F*, additional crude membrane samples were collected to examine GRK2 expression at the PM. *G*, crude PM fraction immunoprecipitation from naive TG from WT AKAP (*black*) mice and AKAP KO (*red*) littermates. *H*, additional crude membrane samples were collected to look at GRK2 expression at the PM. $n = 3$ independent trials; mean $\pm$ S.E. (*error bars*); *, $p < 0.05$; *ns*, not significant; unpaired Student's *t* test.

Because site-specific mutants were used rather than a dominant-negative mutant that would antagonize wild-type GRK2, the abundant native kinase was first knocked down with previously validated GRK2 siRNA (11) (75.9 $\pm$ 1.8 and 78.8 $\pm$ 1.5% endogenous GRK2 reduction for GRK2 siRNA and FITC-GRK2 siRNA, respectively). Following knockdown of endogenous GRK2, we nucleofected either empty vector, wild-type GRK2, GRK2-S685D (phosphomimetic), or GRK2-S685G (phosphodeficient) cDNA into TG cultures. Following overnight serum starvation, cells were harvested, fractionated, and processed for co-immunoprecipitation studies.

Following GRK2 silencing and empty vector introduction, a small amount of native GRK2 co-immunoprecipitates with plasma membrane DOR. When wild-type GRK2 is reconsti-

tuted, constitutive GRK2 association with DOR increases to 149.78 $\pm$ 61.52% above levels in cells nucleofected with empty vector. Introduction of the phosphomimetic mutant, GRK2-S685D, yields a comparable 154.52 $\pm$ 34.23% increase in GRK2 that co-immunoprecipitates with DOR at the plasma membrane. In contrast, introduction of the phosphodeficient mutant, GRK2-S685G, produced a small, non-significant increase of 33.90 $\pm$ 2.96% above levels in GRK2-silenced TG nucleofected with empty vector (Fig. 3*A*; *, $p \leq 0.05$; ANOVA summary, $p = 0.0111$; $n = 4$ independent trials; one-way ANOVA with Bonferroni post hoc test). These data demonstrate that in peripheral sensory neurons, PKA phosphorylation of GRK2 drives the constitutive association between DOR and GRK2 at the plasma membrane.
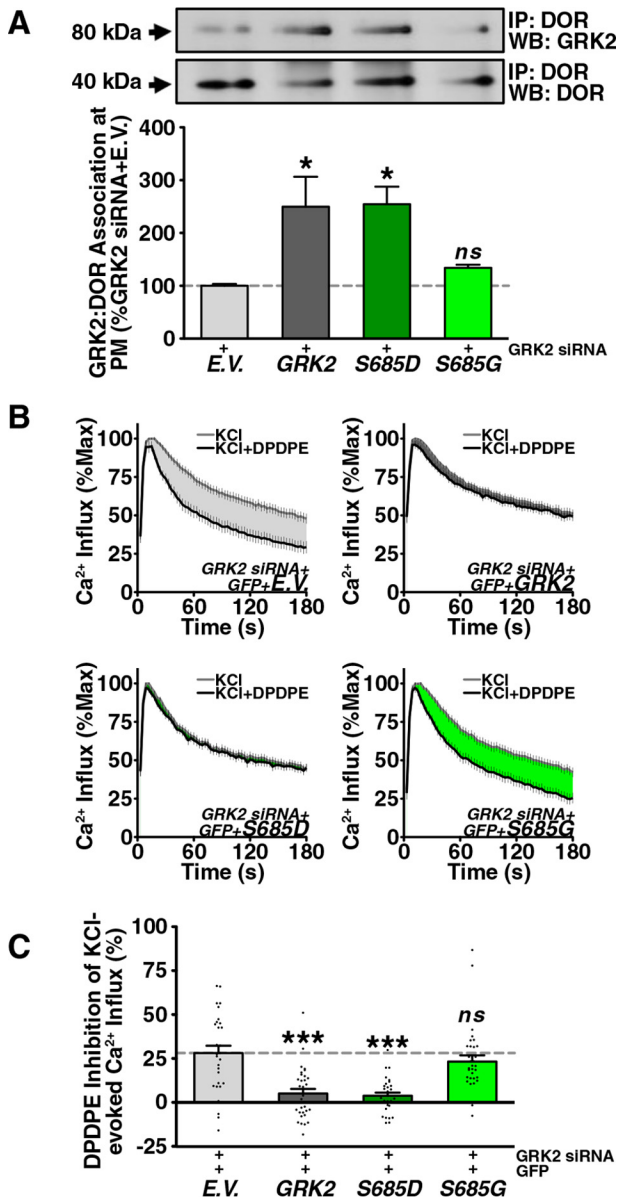
Figure 3. PKA phosphorylation of GRK2 enhances association with DOR in primary sensory neurons of the periphery. *A,* TG cultures were treated with GRK2 siRNA followed by nucleofection of EV (*light gray*), wild-type GRK2 (*dark gray*), phosphomimetic GRK2-S685D (*dark green*), or phosphodeficient GRK2-S685G (*light green*) cDNA. Following 4-h serum starvation, crude plasma membrane fractions were collected for co-immunoprecipitation and probed for DOR association with GRK2. *n* = 4 independent trials; mean ± S.E. (*error bars*); *, *p* < 0.05; *ns*, not significant; one-way ANOVA with Bonferroni post hoc test. *B* and *C*, cumulative traces and quantification of DPDPE (1 μM) inhibition of KCl (50 mM)-evoked Ca^{2+} influx in capsaicin-sensitive DRG treated with GRK2 siRNA followed by co-nucleofection of GFP with EV, GRK2, GRK2-S685D, or GRK2-S685G cDNA and 2-h serum starvation. *n* = 29–33 DRG/group, mean ± S.E.; ***, *p* < 0.005; *ns*, not significant; one-way ANOVA with Bonferroni post hoc test.

To build on this, we next carried out a functional Ca^{2+} imaging assay in peripheral sensory neurons to determine whether PKA-dependent phosphorylation of GRK2 governs DOR incompetence. We measured opioid inhibition of voltage-gated Ca^{2+} channels (VGCCs) elicited by KCl-evoked Ca^{2+} transients in cultured sensory neurons, which is a validated method that has been used by multiple groups to quantify DOR activity in a heterogeneous neuronal population (10, 11, 27). In contrast

to patch-clamp electrophysiology, this method circumvents inevitable user bias in determining whether to include a cell that does not respond to a DOR agonist due to lack of receptor *expression versus* lack of *functional* receptor competence. Furthermore, it avoids the limitations of requiring gene-targeted receptor-fusion protein introduction into cells that do not typically express DOR, which carries with it potential changes to normal receptor activity, interaction partners, and/or biochemistry.

We previously reported that small to medium capsaicin (CAP; 1 μM)-sensitive DRG neurons transfected with FITC-GRK2 siRNA produce significant DOR-mediated inhibition of VGCCs compared with mock-treated cells that have little to no DOR activity in the presence of a DOR agonist (11). To test whether PKA-dependent phosphorylation of GRK2 underlies functional DOR incompetence, we used siRNA-mediated knockdown of GRK2 followed by co-nucleofection of GFP with empty vector, wild-type GRK2, GRK2-S685D, or GRK2-S685G cDNA. Recapitulating published population findings in primary cultures, GFP-positive CAP-sensitive DRG transfected with FITC-GRK2 siRNA and empty vector produce a robust response to the DOR agonist [D-Pen[2,5]]enkephalin (DPDPE; 1 μM), which inhibits KCl (50 mM)-evoked Ca^{2+} transients by 28.10 ± 4.23% in CAP-sensitive DRG (Fig. 3, *B* and *C*). Reintroduction of wild-type GRK2 or nucleofection of GRK2-S685D cDNA similarly antagonizes DPDPE inhibition of KCl-evoked Ca^{2+} transients to 5.48 ± 2.74 and 3.96 ± 1.87%, respectively. However, nucleofection of GRK2-S685G cDNA following GRK2 knockdown results in 25.18 ± 2.92% DPDPE inhibition of KCl-evoked Ca^{2+} transients, similar to DRG transfected with FITC-GRK2 siRNA and empty vector cDNA (Fig. 3, *B* and *C*; ***, *p* < 0.005 for GRK2 and GRK2-S685D compared with both empty vector and GRK2-S685G; ANOVA summary, *p* < 0.0001; *n* = 29–33 DRG/group; one-way ANOVA with Bonferroni post hoc test). Taken together, data presented herein identify that Ser-685 is an important site for GRK2 maintenance of functional DOR incompetence in primary sensory neurons.

AKAP scaffolding of PKA modulates DOR activity via GRK2

Under basal conditions, neuronal AKAP interacts with PKA to promote basal phosphorylation of target proteins and receptors (28). To determine whether AKAP scaffolding of PKA drives GRK2 association with DOR, we utilized overexpression experiments with AKAP wild type and deletion mutants with the PKA- or PKC-binding sequences deleted, termed AKAPΔPKA and AKAPΔPKC (23, 29). In rat TG cultures nucleofected and serum-starved, overexpression of wild-type AKAP, AKAPΔPKA, or AKAPΔPKC results in ~300% endogenous levels observed in whole-cell lysates from cells nucleofected with empty vector (Fig. 4*A*; **, *p* < 0.01; ***, *p* < 0.005; ANOVA summary, *p* < 0.0001; *n* = 4 independent trials; one-way ANOVA with Bonferroni post hoc test). To investigate whether AKAP anchoring of PKA facilitates constitutive GRK2 association with DOR, co-immunoprecipitation experiments were conducted from crude plasma membrane fractions from serum-starved primary TG cultures nucleofected with empty vector, wild-type AKAP, AKAPΔPKA, or AKAPΔPKC cDNAs. As expected, GRK2 co-immunoprecipitates with plasma mem-
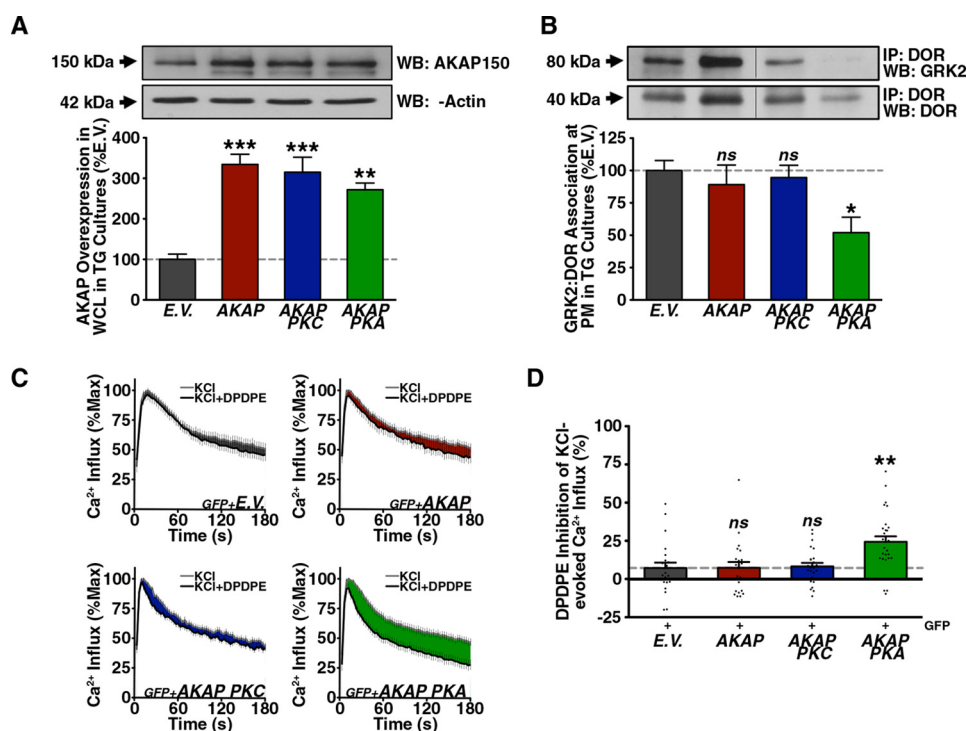
Figure 4. AKAP scaffolding of PKA impairs DOR activity via enhanced GRK2 association with DOR. *A*, AKAP expression in whole-cell lysates from TG cultures nucleofected with EV (*gray*), wild type AKAP (*red*), AKAPΔPKC (*blue*), or AKAPΔPKC (*green*) cDNA. *B*, following 4-h serum starvation, crude plasma membrane fractions were collected for co-immunoprecipitation from each group and probed for DOR association with GRK2. $n = 4$ independent trials; mean ± S.E. (*error bars*); *, $p < 0.05$; ***, $p < 0.005$; *ns*, not significant; one-way ANOVA with Bonferroni post hoc test. Note that representative Western blots have been spliced as indicated. *C* and *D*, cumulative traces and quantification of DPDPE (1 μM) inhibition of KCl (50 mM)-evoked Ca^{2+} influx in capsaicin-sensitive DRG co-nucleofected with GFP and EV, AKAP, AKAPΔPKC, or AKAPΔPKA cDNA and 2-h serum starvation. $n = 22$–29 DRG/group; mean ± S.E.; **, $p < 0.01$; *ns*, not significant; one-way ANOVA with Bonferroni post hoc test.

brane DOR in TG cultures nucleofected with empty vector (Fig. 4*B*). Overexpression of wild-type AKAP or AKAPΔPKC results in similar levels of GRK2 co-immunoprecipitating with DOR in crude plasma membrane fractions. However, in TG cultures overexpressing AKAPΔPKA, 50.40 ± 10.27% less GRK2 co-immunoprecipitates with DOR (Fig. 4*B*; *, $p \leq 0.05$; ANOVA summary, $p = 0.0387$; $n = 4$ independent trials; one-way ANOVA with Bonferroni post hoc test). Thus, the constitutive association between GRK2 and DOR at the plasma membrane is constitutively maintained by AKAP scaffolding of PKA. Surprisingly, overexpression of wild-type AKAP fails to increase DOR-GRK2 association above levels observed in cells expressing endogenous AKAP only. This finding suggests that under basal conditions in peripheral sensory neurons, GRK2 association with DOR is maximally regulated by AKAP-anchored PKA.

To assess whether AKAP scaffolding of PKA supports functional DOR incompetence in primary DRG cultures, we overexpressed GFP with empty vector, wild-type AKAP, AKAPΔPKA, or AKAPΔPKC cDNAs and measured DOR activity in serum-starved neurons. Not surprisingly, GFP-positive CAP-sensitive DRG nucleofected with empty vector were insensitive to DPDPE (1 μM), producing only 7.22 ± 3.58% inhibition of KCl-evoked Ca^{2+} transients (Fig. 4, *C* and *D*). Neither wild-type AKAP overexpression nor AKAPΔPKC-expressing DRG produces significant DPDPE sensitivity at 7.38 ± 3.87 and 8.25 ± 2.40%, respectively. However, GFP-positive CAP-sensitive DRG nucleofected with AKAPΔPKA cDNA produces robust 24.38 ± 3.63% DPDPE inhibition of KCl-evoked Ca^{2+} tran-

sients (Fig. 4, *C* and *D*; *, $p \leq 0.05$; ANOVA summary, $p = 0.0003$; $n = 22$–29 DRG/group; one-way ANOVA with Bonferroni post hoc test). These data demonstrate that under basal conditions, AKAP scaffolding of PKA is a fundamental component in the maintenance of constitutive functional DOR incompetence in primary sensory neurons.

Discussion

In the periphery, DOR lies dormant in an analgesically incompetent state unless primed by inflammation (4, 7–11, 30). Such a prerequisite for receptor activation would be expected to limit the therapeutic efficacy of peripherally restricted DOR agonists to inflammatory pain patients only. However, given the reduced side-effect profiles in rodent and non-human primates following systemic administration, DOR agonists remain an attractive target for the treatment of acute severe pain (2). Recently, we identified a novel, non-internalizing role for GRK2 in chronically down-regulating DOR analgesic competence at the plasma membrane in peripheral sensory neurons as well as peripheral DOR anti-nociception *in vivo* (11). Additionally, we identify a mechanism for DOR priming. However, a major gap in knowledge existed concerning how GRK2 constitutively preserves DOR in an analgesically incompetent state at the plasma membrane in peripheral sensory neurons. The conclusions of the experiments presented in this paper identify this gap (Fig. 5). A working model of the DOR-GRK2 interaction reveals that AKAP scaffolding of PKA constitutively drives PKA-dependent phosphorylation of GRK2 at Ser-685 to increase GRK2 target-

DOR Incompetence in Peripheral Neurons
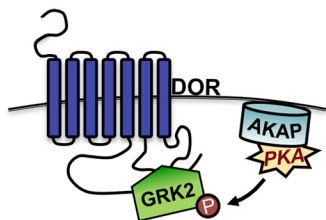
Figure 5. Model of DOR incompetence in peripheral sensory neurons. Under naive conditions, AKAP anchors PKA at the plasma membrane and supports membrane targeting of GRK2 via direct phosphorylation at Ser-685. Constitutive phosphorylation by PKA drives GRK2 to associate with DOR and maintain chronic DOR incompetence.

ing to the plasma membrane, where it interacts with DOR and maintains functional incompetence in primary sensory neurons. Within this framework, novel drugs that disrupt the protein-protein interactions presented herein would be expected to enhance DOR-mediated analgesia.

The results of these experiments are in agreement with studies performed in immortalized cells by Lefkowitz and colleagues (24), who first identified that AKAP scaffolding of PKA indirectly regulates GRK2 by a mechanism that requires PKA tethered to the plasma membrane. The data presented within this work implicate that AKAP expression is essential in constitutive PKA-dependent phosphorylation and membrane targeting of GRK2 in rat peripheral sensory neurons. Although PKA stimulation enhances PKA-dependent phosphorylation of GRK2 at Ser-685 and increases GRK2 targeting to the plasma membrane in serum-starved primary sensory neurons, basal phosphorylation is observed (Fig. 2). Thus, constitutive modulation of GRK2 by PKA could be studied. Following AKAP knockdown, we found noteworthy reductions in GRK2 protein and GRK2 phosphorylation by PKA at the plasma membrane. Although we did not choose to stimulate PKA in this experiment, one would hypothesize that an increase in phosphorylation of GRK2 and targeting to the plasma membrane would be observed following 8-Br-cAMP treatment in the mock-treated cells that would not be observed in the presence of reduced AKAP expression.

In Fig. 3, GRK2 Ser-685, the PKA-dependent phosphorylation site, was identified as an important site for GRK2 maintenance of functional DOR incompetence in primary sensory neurons. In immortalized cells, one might expect that the phosphomimetic GRK2 mutant would have increased association with DOR compared with wild-type GRK2. However, when the potential number of DORs existing at the plasma membrane in a peripheral sensory neuron is compared with the number of GRK2 molecules expected to be present in the cell, it can be presumed that only a fraction of total GRK2 would be needed to maintain DOR incompetence. The data suggest that the amount of DOR at the plasma membrane is maximally associated with GRK2 under naive conditions in primary sensory neurons. In an overexpression system, where additional non-native DOR is introduced, it is likely that much more phosphomimetic GRK2 would be associated with plasma membrane DOR compared with wild-type GRK2. However, this approach was not used because not all peripheral sensory neurons

express DOR. Any implications of such a study would be confounded by introducing DOR into a heterogeneous population of neurons that would not endogenously express the receptor.

It is widely accepted that opioid receptor activation elicits analgesic effects through $G\alpha_i$ and $G\beta\gamma$ subunits, which inhibit neuronal depolarization by inactivating adenylyl cyclase, which reduces cAMP-PKA activity (31), and by inhibiting VGCCs, respectively (32). Thus, it is not surprising that traditional assays for DOR activity in peripheral sensory neurons measure primed DOR agonist inhibition of evoked cAMP accumulation (7, 8, 33, 34). Although constitutive modulation of DOR by PKA has not been investigated in primary sensory neurons, immortalized cell studies suggest that there may be an understudied role for PKA in DOR modulation. In neuroblastoma cells, stimulation of the cAMP-PKA pathway results in down-regulation of DOR transcripts and a loss of radioligand binding sites (35). PKA has been also been implicated in heterologous desensitization of DOR through a mechanism that does not induce receptor internalization or protein down-regulation in immortalized neuroblastoma and stably transfected Chinese hamster ovary cells (36). Whereas PKA is not involved in DOR priming by bradykinin (11), the data presented herein provide compelling evidence that PKA constitutively phosphorylates GRK2 at Ser-685 to maintain functional DOR incompetence in sensory neurons. Although counterintuitive, PKA-dependent phosphorylation of GRK2 does not alter catalytic activity (24). Conspicuously, peripheral DOR analgesic incompetence is independent of GRK2 kinase activity in sensory neurons and, instead, depends on the interaction between the two proteins (11). Catalytic activity of protein kinases has been intensively studied for decades, yet these findings provide accumulating evidence for the diverse non-catalytic functions of kinases.

In conclusion, the experimental results demonstrate that AKAP scaffolding of PKA constitutively dictates PKA-dependent phosphorylation of GRK2 at Ser-685, driving GRK2 to the plasma membrane, where it interacts with DOR to maintain functional incompetence in primary sensory neurons. Prior to this study, there was no identified mechanism underlying chronic GRK2 down-regulation of peripheral DOR analgesic signaling beyond kinase-receptor association. Because this chronic interaction exists to maintain naive peripheral DOR incompetence, novel drugs that disrupt the newly identified protein-protein interactions would be expected to enhance DOR-mediated analgesia in non-inflammatory pain patients for whom DOR agonists would otherwise lack analgesic efficacy.

Experimental procedures

Procedures using animals were approved by the institutional animal care and use committee of the University of Texas Health Science Center at San Antonio and were conducted in accordance with the policies for the ethical treatment of animals established by the National Institutes of Health (NIH). Every effort was made to limit animal discomfort and the number of animals used.

Animals

Adult male Sprague-Dawley rats (Charles River Laboratories, Wilmington, MA) weighing 200–250 g were used for bio-

chemistry and Ca^{2+} imaging in this study. Additional studies in AKAP WT and KO littermates with a C57/B16 background (37) were carried out for immunohistochemistry and biochemistry. Animals were housed in clean cages with a 12-h light/dark cycle for 1 week with food and water *ad libitum* before use.

Generation of PKA phosphorylation site-specific GRK2 mutants

Bovine GRK2 cDNA (generous gift from Dr. Jeffrey L. Benovic (Thomas Jefferson University, Philadelphia, PA) was used for single-point mutational creation of GRK2-S685D (phosphomimetic) and GRK2-S685G (phosphodeficient) in pcDNA3 vector. For GRK2-S685D, a single point mutation changing Ser-685 to aspartic acid was introduced by PCR using the primers 5′-CCA GCG CGG CGA TGC CAA CGG CCT CTG-3′ (forward) and 5′-CAG AGG CCG TTG GCA TCG CCG CGC TGG-3′ (reverse). For GRK2-S685G, a single point mutation changing Ser-685 to glycine was introduced by PCR using the primers 5′-CCA GCG CGG CGG TGC CAA CGG C-3′ (forward) and 5′-GCC GTT GGC ACC GCC GCG CTG G-3′ (reverse). Mutant clones were generated by QuikChange mutagenesis (Stratagene, La Jolla, CA) and then verified by DNA sequencing.

Sensory neuronal cultures

For immunohistochemistry, TG or DRG (L4–L6) were dissected bilaterally from male mice. TG/DRG were dissociated by 30-min collagenase (Worthington) treatment followed by 30-min trypsin (Sigma-Aldrich) treatment, with gentle rocking every 10 min. Cells were then resuspended in complete medium (Dulbecco's modified Eagle's medium, Invitrogen), supplemented with 10% fetal bovine serum (Invitrogen), 100 ng/ml nerve growth factor (NGF; Harlan Laboratories, Indianapolis, IN), mitotic inhibitors (Sigma), 1% penicillin/streptomycin (Invitrogen), and 1% glutamine (Sigma), and plated on poly-D-lysine-coated plates (Corning, Glendale, AZ). Cultures were maintained at 37 °C and 5% CO_2 and grown for 3 days with medium changed 2 days following culture and supplemented with NGF. On the third day post-dissection, cells were prepared for immunofluorescent staining.

For biochemistry, TG were dissected bilaterally from male rats and prepared as described above with cultures maintained at 37 °C and 5% CO_2 and grown for 5–6 days with medium changed the following day and every 2 days thereafter. TG were exclusively utilized for biochemical experiments to satisfy NIH requirements to reduce animal use in research.

For Ca^{2+} imaging, DRG dissected bilaterally at L4–L6 from male rats were dissociated by a 40-min co-treatment with collagenase (Worthington) and dispase (Sigma) with gentle rocking every 10 min. Next, cells were resuspended in complete medium and plated on poly-D-lysine/laminin-coated coverslips (BD Biosciences). Cultures were maintained at 37 °C and 5% CO_2, medium was changed the following day, and experiments were conducted within 24–48 h of initial culture.

Tissue processing and immunohistochemistry

On day 3 post-dissection, wells containing coverslips with cultured sensory neurons from AKAP WT and KO mice were aspirated and rinsed with 0.1 M phosphate-buffered saline (PBS) for three periods of 5 min each. Next, cells were fixed for 10 min in fresh filtered 4% paraformaldehyde solution. Cells were then rinsed quickly once in 0.1 M PBS and again for three periods of 5 min each. To minimize nonspecific binding, samples were incubated for 1 h in blocking solution (2% bovine-globulin (Sigma), 4% normal horse serum (Sigma), and 0.3% Triton X-100 (Fisher) in 0.1 M PBS). Next, the tissue was incubated in primary antibodies against PKA RII (Upstate Cell Signaling Solutions (Lake Placid, NY); at 1:75 dilution in blocking solution) (38) and neuronal/nerve fiber marker protein gene product 9.5 (PGP9.5; AB5898, Chemicon (Billerica, MA); at 1:100 dilution in blocking solution) (39) for 18 h in a humidifier. The following day, cells were rinsed with 0.1 M PBS and then rinsed again for three periods of 10 min each. Next, cells were placed in a dark humidifier for 60 min to incubate in corresponding species-specific secondary antibody Alexa Fluor 488 or 568 (Molecular Probes at dilutions of 1:100 and 1:50, respectively, in blocking solution) used to visualize PKA RII and PGP9.5 immunoreactivity. Cells were quickly rinsed in 0.1 M PBS, followed by an additional three periods of 10 min rinses. Finally, cells were quickly rinsed in ultrafiltered nanopure deionized water. Once dry, stained cells were coverslipped with Vectashield containing DAPI (Vector Laboratories, Burlingame, CA) and stored at 4 °C until they were evaluated by confocal microscopy. Cells were evaluated, and images were obtained using a Nikon 90i microscope equipped with a C1si laser-scanning confocal imaging system (Nikon, Melville, NY). Confocal images are representative of three individual trials.

To analyze PKA RII distribution in each representative cell, a second-order smoothing polynomial of six individual plot profiles measured with 60° separations near the cell membrane was collected under the green filter of the RGB stack using NIH ImageJ software. For every individual plot profile measured under the green filter, a measurement was taken under the red filter to identify distribution constraints for normalization across the cell. PKA RII distribution at the plasma membrane relative to the whole cell was determined using single-pixel-wide segmented measurements selected around the edges of PGP9.5-expressing cells under the red level filter for each cell in every RGB stacked confocal image collected to remove user bias, and PKA RII average densitometry measurements were collected under the green level filter and compared with the average densitometry of the whole cell by closing the segmented line. Appropriate statistics were carried out as described in the figure legends.

Crude membrane preparation

Primary rat TG cultures were pretreated as indicated, and fresh TG from AKAP WT and KO littermates were bilaterally dissected from naive animals. For cultures, cells were harvested and homogenized in homogenization buffer (25 mM HEPES, 25 mM sucrose, 1.5 mM $MgCl_2$, 50 mM NaCl (pH 7.4), 1 mM sodium pyrophosphate, 1 mM sodium orthovanadate (Sigma), 1 μg/ml pepstatin (Sigma), 1 μg/ml leupeptin (Sigma), 1 μg/ml aprotinin (Sigma), and 100 nm phenylmethylsulfonyl fluoride (PMSF; Sigma)) with 20 strokes using a Potter-Elvehjem pestle and glass homogenizer tube. Similarly, naive TG from AKAP

WT and KO littermates were cut 20 times following dissection and then homogenized in homogenization buffer with 40 strokes. Homogenates were placed on ice for a 15-min incubation and then centrifuged at $1000 \times g$ for 1 min to remove nuclei and unlysed cells from the homogenate. The resulting supernatant was centrifuged at $16,000 \times g$ for 30 min at 4 °C to separate cell membrane proteins from cytosolic proteins. Cytosolic supernatant was separated from the pellet (crude membrane fraction), which was resuspended in 250 μl of homogenization buffer containing 1% Triton X-100 (Fisher). Total protein was quantified using Bradford assay (Sigma) prior to co-immunoprecipitation (co-IP).

PKA kinase activity assay/ELISA

Using an *in vitro* PKA kinase activity kit (Enzo Life Sciences, Farmingdale, NY), we measured PKA activity in crude membrane fractions from primary rat TG cultures treated in mock fashion or with AKAP siRNA or fresh TG from AKAP WT and KO littermates. The assay was performed according to the manufacturer's instructions. Following Bradford assay and quantification, 2-μg plasma membrane samples and kit standards were plated onto a precoated 96-well PKA substrate microtiter plate. In brief, ATP was used to initiate the kinase reaction for 90 min at 30 °C. After the reaction was terminated, wells were incubated with a phosphospecific substrate antibody for 60 min at room temperature, when it binds to the phosphorylated peptide substrate. A peroxidase-conjugated secondary antibody that binds the phosphospecific antibody was added for 30 min at room temperature. Finally, a tetramethylbenzidine substrate was added for 45 min at room temperature, and absorbance was measured in a microplate spectrophotometer at 450 nm. A PKA kinase activity assay performed on crude plasma membrane fractions was performed in triplicate across three independent trials for each experiment, as indicated in the corresponding figure legends.

Co-IP/IP

Total protein from either PM or cytosolic fractions was quantified using a Bradford assay (Sigma). For co-IP/IP, equal amounts of protein (125 μg) were immunoprecipitated with 1 μg of anti-GRK2 (C-15, Santa Cruz Biotechnology, Inc.) or anti-DOR (ab66317, Abcam) antiserum. GRK2 antibody specificity has been confirmed in inducible GRK2 sensory neuron knock-out animals (40), and DOR antibody specificity for immunoprecipitation has been previously vetted (41). Protein samples were eluted at 95 °C for 5 min and placed at −20 °C for future WB.

Western blot analysis

Whole cell lysates, PM, and cytosolic immunoprecipitates were resolved on SDS-PAGE (15% gels) and transferred to PVDF membrane (Millipore). Membranes were then blocked with 5% nonfat dried milk in Tris-buffered saline/Tween 20 (TBS-T: 15.35 mM Tris/HCl, 136.9 mM NaCl, pH 7.6, with 0.1% Tween 20) or 5% bovine serum albumin (Sigma) in TBS-T containing the phosphatase inhibitor sodium orthovanadate (1 μM) for phosphorylation-specific antibodies. Western blots were visualized using anti-phospho-GRK2-Ser-685 (catalog no. 12397-1, SAB Signalway Antibody), anti-GRK2 (C-15, Santa Cruz Biotechnology) (40), anti-DOR (ab66317, Abcam) (11, 41, 42), anti-caveolin-1 (N-20, Santa Cruz Biotechnology) (43), or anti-β-actin (I-19-R, Santa Cruz Biotechnology) (43), followed by appropriate horseradish-peroxidase-conjugated secondary antisera (GE Healthcare) and ECL (enhanced chemiluminescence or prime) detection following the manufacturer's protocol (GE Healthcare). Antibody specificities were verified by the manufacturers and BLAST sequence analysis and used in previous publications as indicated. Integrated density measurement values, equivalent to the product of area and mean gray value by histogram analysis, were performed using NIH ImageJ software.

siRNA transfection and cDNA nucleofection

For experiments utilizing AKAP siRNA, cells were transfected with AKAP siRNA (625 ng/10-cm plate; characterized in Ref. 23) for 24 h, and the transfection mix was replaced with complete medium. GRK2 and RKIP siRNA duplexes were transfected into cultured sensory neurons using HiPerFect (Qiagen, Valencia, CA), following the manufacturer's directions. AKAP siRNA yielded a transfection efficiency of ~60–70%, as published previously (23).

For GRK2 siRNA/cDNA nucleofection experiments, primary TG or DRG cultures were transfected with FITC-labeled GRK2 or GRK2 siRNA (45 ng/coverslip; 20 μg/10-cm plate; characterized in Ref. 11) for 18 h, replenished with complete medium. Then 6 h following medium change, cells were nucleofected with Effectene nucleofection reagent (Qiagen) following the manufacturer's instructions, maintaining a cDNA/enhancer reagent ratio of 1:8, for 10 h. For these experiments, empty vector (EV) pcDNA3.1, GRK2 (Dr. Jeffrey L. Benovic, Thomas Jefferson University), GRK2-S685D, or GRK2-S685G cDNA (500 ng/coverslip; 4 μg/10-cm plate) were nucleofected into sensory neurons. For Ca^{2+} imaging, GFP cDNA (250 ng/coverslip) was co-nucleofected to identify positive transfection. GRK2 siRNA yielded a transfection efficiency of ~75%, and nucleofection efficiency was ~60%, as published previously (11). The "rescue" method for reconstituting cDNA following knockdown has been used by multiple groups in human cells (AKAP-Lbc-silenced cryopreserved human cardiomyocytes) (44), zebrafish (GRK2-silenced embryos) (45), and primary sensory neurons (RKIP-silenced TG and DRG) (11).

For AKAP overexpression experiments, DRG were nucleofected with Effectene nucleofection reagent, as described above. Following this protocol, 500 ng/coverslip EV, wild-type AKAP, AKAPΔPKA, or AKAPΔPKC cDNA was co-nucleofected with 250 ng/coverslip GFP cDNA to identify positive transfection. For overexpression of EV, wild-type AKAP, AKAPΔPKA, or AKAPΔPKC cDNA in TG or DRG cultures, 4 μg of cDNA were nucleofected onto 10-cm plates following the same protocol.

Ca^{2+} imaging

Fura-2 AM was used to image individual neurons within a population of cultured DRG following 2-h serum starvation. Next, cells were loaded with fura-2 AM (1 μM; Molecular Probes, Carlsbad, CA) with pluronic F-127 (0.04%; Molecular

Probes) and incubated for 1 h at 37 °C in the dark, in standard extracellular solution (SES) containing 140 mM NaCl, 5 mM KCl, 2 mM CaCl$_2$, 1 mM MgCl$_2$, 10 mM HEPES, 10 mM D-(+)-glucose, pH 7.40. Cells were viewed on an inverted Nikon Eclipse T$_i$-U microscope fitted with a ×20/0.75 numerical aperture Fluor objective and imaged using the MetaFluor system for ratio fluorescence (MetaMorph, Downingtown, PA). Fluorescent images were taken alternately every 3 s with 340- and 380-nm excitation wavelengths in combination with a 510-nm emission filter with 100-ms exposure. The ratio of ΔF340/F380 was plotted for each cell *versus* time. Intracellular Ca^{2+} levels were analyzed as ΔF340/F380 ratios background-corrected and normalized to the initial value, R_0. Corresponding filters were used to select FITC siRNA- and/or GFP-positive DRG.

DOR activity in sensory neurons was quantified by Ca^{2+} imaging as a measure of DPDPE (1 μM; Sigma) inhibition of KCl-evoked Ca^{2+} transients in CAP-sensitive DRG (11). For positive neuronal identification, specific criteria were used and included 1) characteristic phenotype featuring bright round cell bodies with clear nuclei (26, 46); 2) sensitivity to depolarizing solution of 50 mM KCl (10, 27), and 3) sensitivity to CAP (1 μM, 25% above baseline (11); Sigma) to indicate positive sensory neuronal phenotype within a heterogeneous culture.

For each cell imaged, basal Ca^{2+} levels were recorded for 60 s. A perfusion valve controller (< 0.1 p.s.i.) and multibarrel glass pipette were used to apply 3-s exposures of 50 mM KCl at five time points: 60, 270, 740, 950, and 1440 s. The first and second exposures to KCl were given in the absence of a DOR agonist in SES bath solution. At 480 s, SES was replaced with a DPDPE in SES applied via constant perfusion (< 0.1 p.s.i.) by a multibarrel glass pipette. Prior to the third and fourth exposure to KCl, DOR agonist microinjection was terminated to reduce pressure-related artifacts. At 1160 s, SES containing DOR agonist was washed out and replaced with SES via bath perfusion (< 0.1 p.s.i.) using an ML-6 manifold apparatus prior to the fifth exposure to KCl. Finally, cells were exposed to 1 μM CAP at 1770 s to select for TRPV1-positive primary afferent neurons that can be correlated with thermal allodynia behavior.

In order to measure DPDPE inhibition of KCl-evoked Ca^{2+} influx, single-cell recording traces were used to obtain the average area under the curve, calculated as an integral over a time period (3 min) for the average cellular response to KCl in the absence or presence of a DOR agonist. The following equations were used to calculate DOR activity.

$$\text{KCl} = \frac{(\text{KCl}_1, \ \text{KCl}_2, \ \text{KCl}_5)}{3} \quad \text{(Eq. 1)}$$

$$\text{KCl} + \text{DPDPE} = \frac{(\text{KCl}_3, \ \text{KCl}_4)}{2} \quad \text{(Eq. 2)}$$

$$\text{DPDPE agonist inhibition (\%)} = 100 \\ - \left(\frac{\text{AUC}_{\text{KCl+DPDPE}}}{\text{AUC}_{\text{KCl}}} \times 100\% \right) \quad \text{(Eq. 3)}$$

For Ca^{2+} imaging, stock solutions of DOR agonist DPDPE (1 mM) were prepared in sterile water. CAP (1 mM) stock solution

was prepared in EtOH. KCl was prepared fresh in SES on the day of experimentation. All drugs and appropriate vehicles were diluted in SES.

Statistics

GraphPad Prism version 5.0 was used for statistical analyses (GraphPad Software, Inc., La Jolla, CA). Quantitative data are expressed as means ± S.E. Statistical significance was determined by Student's unpaired *t* test, one-way ANOVA, or two-way ANOVA with Bonferroni post hoc analyses as needed. $p < 0.05$ was considered statistically significant.

References

1. Højsted, J., and Sjøgren, P. (2007) Addiction to opioids in chronic pain patients: a literature review. *Eur. J. Pain* **11,** 490–518
2. Vanderah, T. W. (2010) δ and κ opioid receptors as suitable drug targets for pain. *Clin. J. Pain* **26,** S10–S15
3. Stein, C. (2013) Targeting pain and inflammation by peripherally acting opioids. *Front. Pharmacol.* **4,** 123
4. Stein, C., Millan, M. J., Shippenberg, T. S., Peter, K., and Herz, A. (1989) Peripheral opioid receptors mediating antinociception in inflammation. Evidence for involvement of μ, δ and κ receptors. *J. Pharmacol. Exp. Ther.* **248,** 1269–1275
5. Przewłocki, R., and Przewłocka, B. (2001) Opioids in chronic pain. *Eur. J. Pharmacol.* **429,** 79–91
6. Stein, C., Machelska, H., Binder, W., and Schäfer, M. (2001) Peripheral opioid analgesia. *Curr. Opin. Pharmacol.* **1,** 62–65
7. Patwardhan, A. M., Berg, K. A., Akopian, A. N., Jeske, N. A., Gamper, N., Clarke, W. P., and Hargreaves, K. M. (2005) Bradykinin-induced functional competence and trafficking of the δ-opioid receptor in trigeminal nociceptors. *J. Neurosci.* **25,** 8825–8832
8. Patwardhan, A. M., Diogenes, A., Berg, K. A., Fehrenbacher, J. C., Clarke, W. P., Akopian, A. N., and Hargreaves, K. M. (2006) PAR-2 agonists activate trigeminal nociceptors and induce functional competence in the δ opioid receptor. *Pain* **125,** 114–124
9. Rowan, M. P., Ruparel, N. B., Patwardhan, A. M., Berg, K. A., Clarke, W. P., and Hargreaves, K. M. (2009) Peripheral δ opioid receptors require priming for functional competence *in vivo. Eur. J. Pharmacol.* **602,** 283–287
10. Pettinger, L., Gigout, S., Linley, J. E., and Gamper, N. (2013) Bradykinin controls pool size of sensory neurons expressing functional δ-opioid receptors. *J. Neurosci.* **33,** 10762–10771
11. Brackley, A. D., Gomez, R., Akopian, A. N., Henry, M. A., and Jeske, N. A. (2016) GRK2 constitutively governs peripheral δ opioid receptor activity. *Cell Rep.* **16,** 2686–2698
12. Corbin, J. D., Soderling, T. R., and Park, C. R. (1973) Regulation of adenosine 3′,5′-monophosphate-dependent protein kinase. *J. Biol. Chem.* **248,** 1813–1821
13. Corbin, J. D., and Keely, S. L. (1977) Characterization and regulation of heart adenosine 3′:5′-monophosphate-dependent protein kinase isozymes. *J. Biol. Chem.* **252,** 910–918
14. Potter, R. L., and Taylor, S. S. (1979) Relationships between structural domains and function in the regulatory subunit of cAMP-dependent pro-

ASBMB

J. Biol. Chem. (2017) 292(21) 8762–8772 **8771**

tein kinases I and II from porcine skeletal muscle. *J. Biol. Chem.* **254,** 2413–2418

15. Corbin, J. D., Keely, S. L., and Park, C. R. (1975) The distribution and dissociation of cyclic adenosine 3′:5′-monophosphate-dependent protein kinases in adipose, cardiac, and other tissues. *J. Biol. Chem.* **250,** 218–225

16. Lee, D. C., Carmichael, D. F., Krebs, E. G., and McKnight, G. S. (1983) Isolation of cDNA clone for the type I regulatory subunit of bovine cAMP-dependent protein kinase. *Proc. Natl. Acad. Sci. U.S.A.* **80,** 3608–3612

17. Scott, J. D., Glaccum, M. B., Zoller, M. J., Uhler, M. D., Helfman, D. M., McKnight, G. S., and Krebs, E. G. (1987) The molecular cloning of a type II regulatory subunit of the cAMP-dependent protein kinase from rat skeletal muscle and mouse brain. *Proc. Natl. Acad. Sci. U.S.A.* **84,** 5192–5196

18. Carr, D. W., Hausken, Z. E., Fraser, I. D., Stofko-Hahn, R. E., and Scott, J. D. (1992) Association of the type II cAMP-dependent protein kinase with a human thyroid RII-anchoring protein cloning and characterization of the RII-binding domain. *J. Biol. Chem.* **267,** 13376–13382

19. Glantz, S. B., Li, Y., and Rubin, C. S. (1993) Characterization of distinct tethering and intracellular targeting domains in AKAP75, a protein that links cAMP-dependent protein kinase II β to the cytoskeleton. *J. Biol. Chem.* **268,** 12796–12804

20. Lu, Y., Allen, M., Halt, A. R., Weisenhaus, M., Dallapiazza, R. F., Hall, D. D., Usachev, Y. M., McKnight, G. S., and Hell, J. W. (2007) Age-dependent requirement of AKAP150-anchored PKA and GluR2-lacking AMPA receptors in LTP. *EMBO J.* **26,** 4879–4890

21. Weisenhaus, M., Allen, M. L., Yang, L., Lu, Y., Nichols, C. B., Su, T., Hell, J. W., and McKnight, G. S. (2010) Mutations in AKAP5 disrupt dendritic signaling complexes and lead to electrophysiological and behavioral phenotypes in mice. *PLoS One* **5,** e10325

22. Sanderson, J. L., Gorski, J. A., and Dell'Acqua, M. L. (2016) NMDA receptor-dependent LTD requires transient synaptic incorporation of Ca^{2+}-permeable AMPARs mediated by AKAP150-anchored PKA and calciuneurin. *Neuron* **89,** 1000–1015

23. Jeske, N. A., Diogenes, A., Ruparel, N. B., Fehrenbacher, J. C., Henry, M., Akopian, A. N., and Hargreaves, K. M. (2008) A-kinase anchoring protein mediates TRPV1 thermal hyperalgesia through phosphorylation of TRPV1. *Pain* **138,** 604–616

24. Cong, M., Perry, S. J., Lin, F. T., Fraser, I. D., Hu, L. A., Chen, W., Pitcher, J. A., Scott, J. D., and Lefkowitz, R. J. (2001) Regulation of membrane targeting of the G protein-coupled receptor kinase 2 by protein kinase A and its anchoring protein AKAP79. *J. Biol. Chem.* **276,** 15192–15199

25. Carr, D. W., Stofko-Hahn, R. E., Fraser, I. D., Cone, R. D., and Scott, J. D. (1992) Localization of the cAMP-dependent protein kinase to the postsynaptic densities by A-kinase anchoring proteins: characterization of AKAP 79. *J. Biol. Chem.* **267,** 16816–16823

26. Liu, R., Lin, G., and Xu, H. (2013) An efficient method for dorsal root ganglia neurons purification with a one-time anti-mitotic reagent treatment. *PLoS One* **8,** e60558

27. Khasabova, I. A., Harding-Rose, C., Simone, D. A., and Seybold, V. S. (2004) Differential effects of CB1 and opioid agonists on two populations of adult rat dorsal root ganglion neurons. *J. Neurosci.* **24,** 1744–1753

28. Tavalin, S. J., Colledge, M., Hell, J. W., Langeberg, L. K., Huganir, R. L., and Scott, J. D. (2002) Regulation of GluR1 by the A-kinase anchoring protein 79 (AKAP79) signaling complex shared properties with long-term depression. *J. Neurosci.* **22,** 3044–3051

29. Jeske, N. A., Patwardhan, A. M., Ruparel, N. B., Akopian, A. N., Shapiro, M. S., and Henry, M. A. (2009) A-kinase anchoring protein 150 controls protein kinase C-mediated phosphorylation and sensitization of TRPV1. *Pain* **146,** 301–307

30. Gavériaux-Ruff, C., Karchewski, L. A., Hever, X., Matifas, A., and Kieffer, B. L. (2008) Inflammatory pain is enhanced in δ opioid receptor-knockout mice. *Eur. J. Neurosci.* **27,** 2558–2567

31. Law, P. Y., and Bergsbaken, C. (1995) Properties of δ opioid receptor in neuroblastoma NS20Y: receptor activation and neuroblastoma proliferation. *J. Pharmacol. Exp. Ther.* **272,** 322–332

32. Ford, C. E., Skiba, N. P., Bae, H., Daaka, Y., Reuveny, E., Shekter, L. R., Rosal, R., Weng, G., Yang, C. S., Iyengar, R., Miller, R. J., Jan, L. Y., Lefkowitz, R. J., and Hamm, H. E. (1998) Molecular basis for interactions of G protein βγ subunits with effectors. *Science* **280,** 1271–1274

33. Breit, A., Gagnidze, K., Devi, L. A., Lagacé, M., and Bouvier, M. (2006) Simultaneous activation of the δ opioid receptor (δOR)/sensory neuron-specific receptor-4 (SNSR-4) hetero-oligomer by the mixed bivalent agonist bovine adrenal medulla peptide 22 activates SNSR-4 but inhibits δOR signaling. *Mol. Pharmacol.* **70,** 686–696

34. Berg, K. A., Rowan, M. P., Gupta, A., Sanchez, T. A., Silva, M., Gomes, I., McGuire, B. A., Portoghese, P. S., Hargreaves, K. M., Devi, L. A., and Clarke, W. P. (2012) Allosteric interactions between δ and κ opioid receptors in peripheral sensory neurons. *Mol. Pharmacol.* **81,** 264–272

35. Buzas, B., Rosenberger, J., and Cox, B. M. (1997) Regulation of δ-opioid receptor mRNA levels by receptor-mediated and direct activation of the adenylyl cyclase-proetin kinase A pathway. *J. Neurochem.* **68,** 610–615

36. Xu, W., Chen, C., Li, J. G., Dimattio, K., Wang, Y., Unterwald, E., and Liu-Chen, L. Y. (2013) PKA and ERK1/2 are involved in dopamine D$_1$ receptor induced heterologous desensitization of the δ opioid receptor. *Life Sci.* **92,** 1101–1109

37. Tunquist, B. J., Hoshi, N., Guire, E. S., Zhang, F., Mullendorff, K., Langeberg, L. K., Raber, J., and Scott, J. D. (2008) Loss of AKAP150 perturbs distinct neuronal processes in mice. *Proc. Natl. Acad. Sci. U.S.A.* **105,** 12557–12562

38. Reynolds, J. G., McCalmon, S. A., Tomczyk, T., and Naya, F. J. (2007) Identification and mapping of protein kinase A binding sites in the costameric protein myospryn. *Biochim. Biophys. Acta* **1773,** 891–902

39. Alvarado, L. T., Perry, G. M., Hargreaves, K. M., and Henry, M. A. (2007) TRPM8 axonal expression is decreased in painful human teeth with irreversible pulpitis and cold hyperalgesia. *J. Endod.* **33,** 1167–1171

40. Wang, H., Heijnen, C. J., Eijkelkamp, N., Garza Carbajal, A., Schedlowski, M., Kelley, K. W., Dantzer, R., and Kavelaars, A. (2011) GRK2 in sensory neurons regulates epinephrine-induced signalling and duration of mechanical hyperalgesia. *Pain* **152,** 1649–1658

41. Rowan, M. P., Szteyn, K., Doyle, A. P., Gomez, R., Henry, M. A., and Jeske, N. A. (2014) β-Arrestin-2-biased agonism of δ opioid receptors sensitizes transient receptor potential vanilloid type 1 (TRPV1) in primary sensory neurons. *Mol. Pain* **10,** 50

42. Byun, S. W., Chang, Y. J., Chung, I. S., Moss, S. F., and Kim, S. S. (2012) *Helicobacter pylori* decreases p27 expression through the δ opioid receptor-mediated inhibition of histone acetylation within the p27 promoter. *Cancer Lett.* **326,** 96–104

43. Gomez, R., Por, E. D., Berg, K. A., Clarke, W. P., Glucksman, M. J., and Jeske, N. A. (2011) Metallopeptidase inhibition potentiates bradykinin-induced hyperalgesia. *Pain* **152,** 1548–1554

44. Edwards, H. V., Scott, J. D., and Baillie, G. S. (2012) The A-kinase-anchoring protein AKAP-Lbc facilitates cardioprotective PKA phosphorylation of Hsp20 on Ser(16). *Biochem. J.* **446,** 437–443

45. Zhao, Z., Lee, R. T., Pusapati, G. V., Iyu, A., Rohatgi, R., and Ingham, P. W. (2016) An essential role for GRK2 in Hedgehog signaling downstream of Smoothened. *EMBO Rep.* **17,** 739–752

46. Goldenberg, S. S., and De Boni, U. (1983) Pure population of viable neurons from rabbit dorsal root ganglia, using gradients of Percoll. *J. Neurobiol.* **14,** 195–206